IOPscience iopscience.iop.org

Home Search Collections Journals About Contact us My IOPscience

Defects in sublimation-grown SiC bulk crystals

This article has been downloaded from IOPscience. Please scroll down to see the full text article.

2002 J. Phys.: Condens. Matter 14 13009

(http://iopscience.iop.org/0953-8984/14/48/345)

View the table of contents for this issue, or go to the journal homepage for more

Download details:
IP Address: 171.66.16.97
The article was downloaded on 18/05/2010 at 19:14

Please note that terms and conditions apply.

INSTITUTE OF PHYSICS PUBLISHING JOURNAL OF PHYSICS: CONDENSED MATTER

J. Phys.: Condens. Matter **14** (2002) 13009–13018 PII: S0953-8984(02)54090-X

Defects in sublimation-grown SiC bulk crystals

Roland Madar[1], Etienne Pernot[1], Mikael Anikin[1] and Michel Pons[2]

[1] Institut National Polytechnique de Grenoble, Laboratoire de Matériaux et de Génie Physique, UMR CNRS/INPG 5628-ENSPG, BP 46, 38402 Saint Martin D'Heres, France
[2] Laboratoire de Thermodynamique et Physicochimie Métallurgiques, UMR CNRS/INPG/UJF 5614, Enseeg, BP 75, 38402 Saint Martin D'Heres, France

Received 27 September 2002
Published 22 November 2002
Online at stacks.iop.org/JPhysCM/14/13009

Abstract

In view of its excellent thermal, mechanical and electronic properties, silicon carbide is the reference semiconductor material for high-temperature, high-frequency and high-power devices.

Ingots of monocrystalline SiC which are currently grown by the seeded sublimation growth technique have opened the path to the production of large-area SiC wafers. Despite constant progress in crystal growth, the development of industrial applications has been up to now severely limited by the insufficient quality and size of the substrates. This situation results mainly from the fact that the growing process is quite complex. As a consequence, it is quite difficult to control the growth of a given polytype and the doping level while decreasing the number of defects such as misoriented domains, inclusions, macrodefects and micropipes.

This paper is mainly devoted to a review of our work on the influence of the seed characteristics and the growth process parameters, such as the thermal field and the pressure, on the occurrence of defects in the as grown ingot and on the enlargement process. Polytype identification and morphology, structural perfection and defect analyses have been carried out using mainly polarized light microscopy and x-ray white-beam synchrotron topography.

1. Introduction

Wide-bandgap semiconductors are considered to be the materials of the future in the electronics field. The specific properties of these semiconductors, such as diamond, silicon carbide, gallium nitride and aluminium nitride, make them likely candidates for use in the fabrication of electronic devices that perform better than silicon at high temperatures, high frequencies and high powers. SiC was one of the first semiconductor materials discovered, and is by far the most developed of the wide-bandgap materials. Although the semiconducting properties of SiC have been known for a long time, numerous technological obstacles have hindered any fast electronic development based on silicon carbide. Until recently (Tsvetkov *et al* 1998, Müller

et al 2000), the lack of suitable SiC crystal growth processes was the key factor preventing the commercialization of SiC devices. Growth of bulk single crystal is complex for two main reasons. The first one concerns its stability. SiC does not melt under reasonable pressure: rather it sublimes, incongruently, at temperature greater than 2000 K. Growth from melt techniques massively used for the fabrication of silicon and GaAs are consequently not applicable. The second one comes from the multiplicity of polytypes: about 175 are known. Each of them has different electronic characteristics and can grow under apparently identical conditions. Only 6H and 4H polytypes are now commercially available. In this paper, our recent results concerning the nature and occurrence of defects, in relation with the various parameters of SiC bulk growth technology, are summarized. Different characterization techniques, in particular x-ray topography, were used to visualize the nature of the polytypes, stress and structural defects such as dislocations or subgrain boundaries. The aim of this paper is to describe some trends in the relations between growth conditions, defect formations and ingot shapes.

2. Experimental details

2.1. Crystal growth

6H and 4H crystals with diameter up to 40 mm have been grown by the modified Lely method with '*in situ*' sublimation etching (Tairov and Tsvetkov 1978, Anikin and Madar 1997, Tsvetkov *et al* 1998, Chourou *et al* 1998). An experimental set-up with RF heating and a graphite crucible was used. The crucible was wrapped by graphite felt for thermal insulation and the whole assembly was placed inside a water-cooled quartz reactor. The growth temperature was about 2200 °C and the argon pressure was about 2 Torr. Under these experimental conditions we obtained 4H and 6H single crystals with a thickness of about 10 mm. The growth rate was between 0.8 and 1.1 mm h^{-1}.

The seeds used were on-axis 6H-SiC Lely crystals and 8° off-axis 4H-SiC wafers from a previous growth process. The seed was fixed on the lid at the top of the crucible. The distance between source and seed was in the range 15–20 mm. The temperature gradient within the growth cell was continuously changed during the growth process. First, etching of the seed was performed by inverting the temperature gradient.

The as-obtained monocrystalline ingots of cylindrical shape were surrounded by polycrystalline SiC deposited on the uncovered graphite part of the lid. The ingot surface is almost flat or weakly convex and the orientation of the 6H-SiC and 4H-SiC ingots is on-axis and 8° off-axis respectively.

2.2. Crystal evaluation; characterization techniques

To improve the crystalline quality of SiC wafer grown by the modified Lely method, it is necessary to identify the defects and to evaluate their density. For that, several methods were used. The polytype identification is generally made by means of x-ray diffraction and Raman spectroscopy. The crystal defect densities and distribution are assessed by x-ray diffraction imaging, also called x-ray topography, and polarized light microscopy.

Optical microscopy; the polarized light technique. Wafers cut from the as-grown ingot are characterized by optical microscopy using white light. The transmission micrographs are recorded using a polarizing microscope with a crossed analyser. This technique allows one to reveal strains accompanying micropipes and grain boundaries via the photo-elastic effect or polytype inclusions corresponding to different refractive index values.

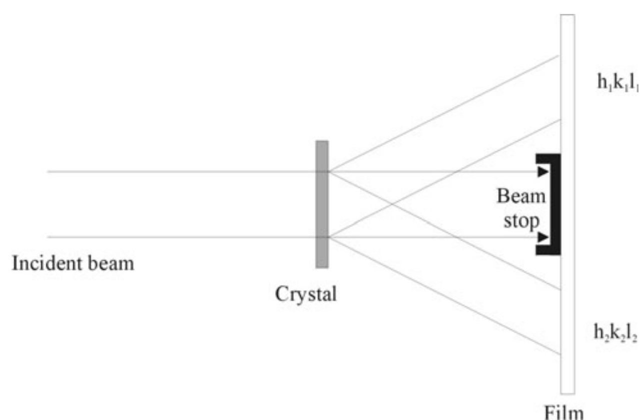

Figure 1. A sketch of the experimental set-up for white-beam synchrotron topography in transmission mode.

X-ray diffraction imaging (also called topography). In the white-beam synchrotron diffraction imaging (Baruchel *et al* 1994, Authier *et al* 1996), the most commonly used topographic technique in this paper, the sample is just placed into the beam without the need for exact adjustments. Many lattice planes will meet the reflection condition and form a Laüe pattern, so several topographs can be simultaneously recorded within one exposure on the film; see figure 1. In the samples investigated, it is easy to identify the contrast coming from dislocations, inclusions and disorientations.

The diffraction section topographic technique allows the visualization of deformations and misorientations within a 'virtual' slice of a single crystal by restricting the incident beam width in one direction using the slit. A sketch of the experimental set-up is shown in figure 2(a). In the case of very thick samples (thickness of a few centimetres), this is a simple way to avoid the projection of a huge crystal volume onto a two-dimensional detector. This projection is primarily useful if the crystalline quality of the sample investigated is not very high, like in the SiC case when compared with industrial Si crystal.

The section topographs recorded at the different positions of the incident beam on the sample together with the use of four distinct geometries, schematically depicted in figure 2, allow the determination of the three-dimensional shape of defects inside the ingot. In the case of 4H-SiC, due to the 8° off-axis orientation of the seed, the growth is not symmetric and it is useful to record topographs with four positions with respect to the axis of the growth.

The 'horizontal' sections were taken with the main axis of a cylindrical ingot vertical and the *c*-axis (perpendicular to the facet visible on the top of each ingot) pointed upwards and to the left with respect to the incident beam direction; see figures 2(a) and (b) respectively. Accordingly, the horizontal sections correspond to the areas of the ingot formed approximately at the same moment of crystal growth.

The 'vertical' sections were taken with the main ingot axis lying along the incident beam direction and with the *c*-axis pointed upwards and to the left with respect to it; see figures 2(c) and (d), respectively. The vertical sections allow one to visualize the seed–crystal interface and the propagation of a given defect during the crystal growth.

To study growth from on-axis seeds, like 6H-SiC, only one horizontal geometry and one of the vertical geometries were used, the facet being at the centre of the ingot.

The experiments were performed using synchrotron radiation at the ID19 and BM5 beamlines at the European Synchrotron Radiation Facility (Grenoble, France). The topographs

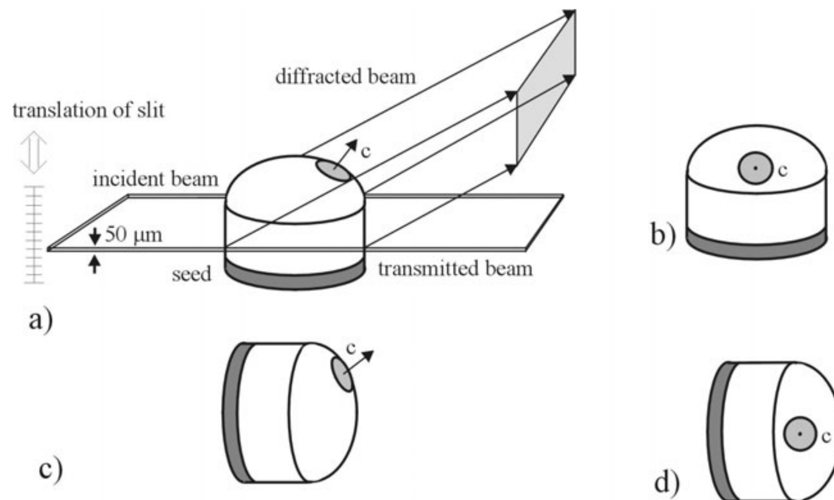

Figure 2. The experimental arrangement for section topography on an off-axis ingot with the possibility of modifying the incident beam position on the sample by displacement of the slit. Four geometries of an ingot with respect to the facet perpendicular to the *c*-axis are presented and called horizontal (a) and (b) and vertical (c) and (d) sections.

in white-beam mode were recorded as Laüe patterns on Kodak Industrex SR films with a typical exposure time between 0.1 and 30 s and a crystal-to-film distance between 20 and 40 cm. The spatial resolution is about 5 μm.

3. Results

For a given growth rate of the single-crystal ingot, grown in the standard configuration of figure 3(a), the crystal quality and defect occurrence are mainly functions of two parameters of the growth process: the seed characteristics and the thermal field inside the growth chamber.

3.1. Seed characteristics: surface polarity and polytype

It has been already reported that 4H-SiC and 6H-SiC ingots can be preferentially grown by the modified Lely method respectively on the C face of 4H-SiC and on both the C and the Si faces of 6H-SiC seed crystals. Polytypic conversions may occur when the face polarity is not respected. A 4H-SiC ingot grown from a Si face often changes to 6H polytype, while 6H- or 15R-SiC polytypes can be grown on the C face of a 6H-SiC seed (Schulze *et al* 1999).

Milita *et al* (1998) have already reported analyses by white-beam vertical section topography of a 6H-SiC ingot grown on the Si face of a Lely seed. So, in this case the seed is on-axis and the geometries of figures 2(c) and (d) for the vertical sections are the same. The interface between the seed and the grown crystal has been observed. Figure 4 shows the result of the same experiment performed on an ingot grown on the C face of a Lely seed. The seed diffracted at the top of the topograph and the as-grown ingot surface diffracted at the bottom. In this case, in contrast to what has been observed previously by Milita *et al* (1998), the seed/grown crystal interface is highly perturbed. Moreover, a small inclusion at the interface can be identified by analysing the whole film. Indeed, figure 4 shows, between the Lely seed and the grown crystal, a small white line corresponding to an inclusion of another polytype which did not diffract at the same angle as the 6H crystal. On the other hand, a small

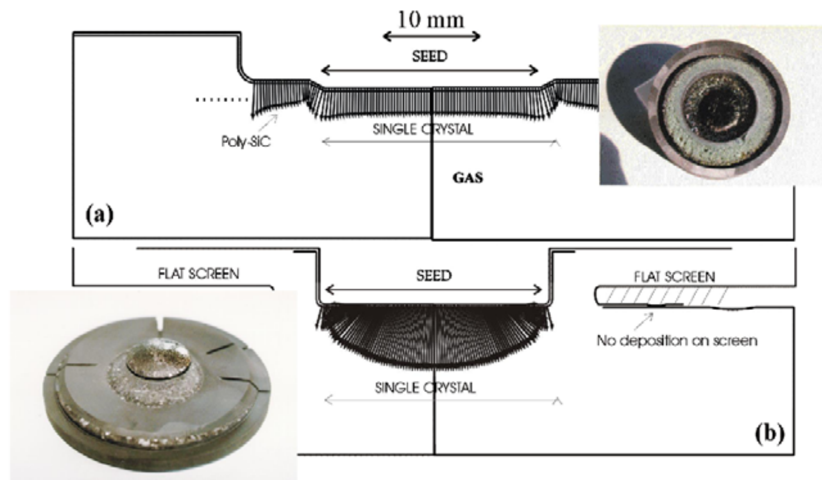

Figure 3. Initial growth flux for (a) a standard configuration and (b) a configuration with a flat screen inserted in the cavity.

(This figure is in colour only in the electronic version)

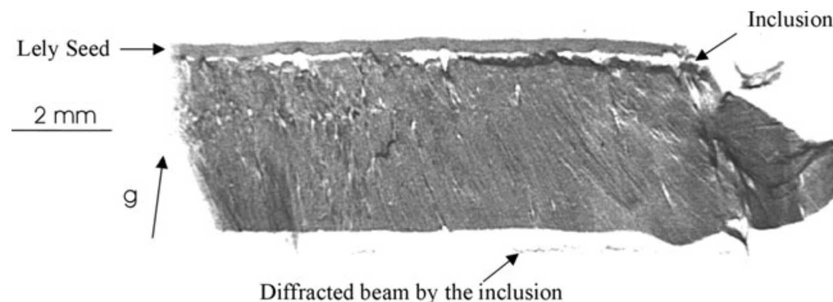

Figure 4. A vertical section of a 6H-SiC ingot. The C face of an on-axis Lely crystal was used to grow this ingot. In this case the two geometries of the vertical section are same.

dark line is visible at the bottom of figure 4 which probably comes from this inclusion. The polytype 15R-SiC has been identified by Raman spectroscopy. It has been already observed that 6H/15R-SiC conversion often occurs when the growth takes place on the C face of a 6H seed. This is also probably the case here. A small 15R-SiC inclusion is grown on the seed and returns to 6H-SiC, which is more stable in our growth conditions, after less than 1 mm of growth. The low crystalline quality of this 6H-SiC ingot must also be noted.

This observation confirms that the growth of the 6H polytype is difficult if the growth occurs on the C face of a seed. But the fact that the main part of the grown ingot is 6H-SiC means that for our experimental conditions, pressure and temperature, the 6H polytype is the thermodynamically stable structure.

3.2. Thermal field

Enlargement process. In the simplest experimental configuration the growth starts simultaneously on the SiC seed, the pedestal part not covered by the seed and the remaining surface of the lid. At first, on these last two graphite surfaces, the SiC deposit is essentially polycrystalline.

Figure 5. A vertical section (D-geometry) of a 4H-SiC ingot showing the enlargement of the crystal during the growth. The seed is at the upper level.

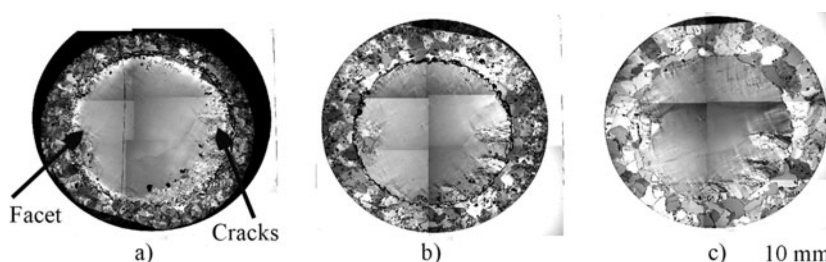

Figure 6. Polarized light microscopy of three wafers cut from the same ingot: (a) near the seed, b) in the middle of the ingot and (c) near the as-grown surface.

This enlargement process has been studied by white-beam synchrotron topography. We will just give here some indications on the main information obtained to date. The investigation of a SiC boule by horizontal and vertical section topography reveals that the enlargement process results from a progressive alignment of domains adjacent to the seed and initially disoriented by a continuous deformation of the boundary zones during the growth. A complete description and analysis of the results obtained so far by this technique have been published elsewhere together with a comparison with the work already published on this subject (Madar *et al* 1997, Milita *et al* 1998, Moulin *et al* 2001).

Figure 5 shows a vertical section topograph of a 4H-SiC ingot. A better quality in the centre of the boules (the lighter region) can be noted. The darker regions are essentially observable at the edge of the boule and at the beginning of the growth. The central part of the crystal under the seed retains the good structural quality of the seed, whereas the enlarged part coming from the alignment of the polycrystal is more stressed.

Heat transfer modelling provides a good understanding of this enlargement phenomenon based on the radial gradient along the growth surface. Due to this radial gradient, ingot diameter increases with increase in length if the growth of the polycrystalline SiC on the graphite lid follows the ingot growth. An increase in radial gradient increases the lateral growth rate.

Growth of the polycrystal and cracks. The defect propagation and the evolution of the polycrystalline part around the single-crystal ingot have been investigated by polarized light microscopy. Figure 6 shows the optical micrographs of three 4H-SiC slices cut from the same ingot close to the seed, at the middle of the ingot and close to the as-grown surface. The design of the growth chamber was such that there is no enlargement of the ingot. Its size was $\varnothing 20 \times 7$ mm.

Some polycrystal has grown around the main crystal. Near the seed, the grain size is very small. Probably because of a particular orientation, some grains grow from the seed level to the top of the ingot. It has been shown (Madar *et al* 1997, Milita *et al* 1998) that some crystallites in the polycrystal have a common axis and an orientation similar to that of the main crystal. In the case of an enlargement process, these crystallites formed subgrains which gradually join the main crystal.

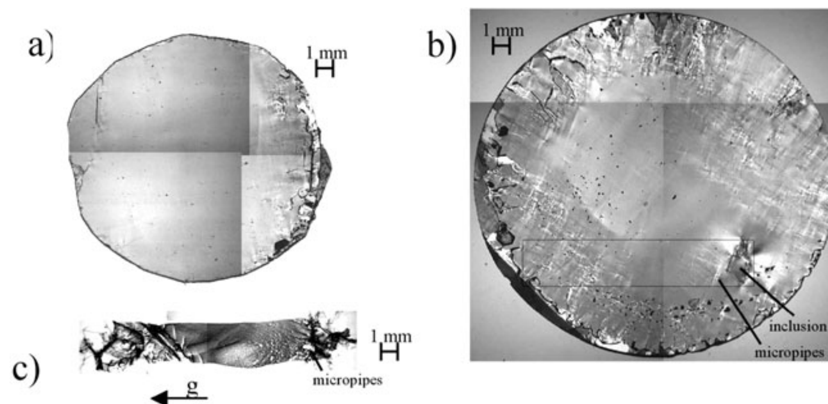

Figure 7. Optical transmission micrographs recorded using the polarizing microscope with a crossed analyser of (a) the seed wafer and (b) the wafer cut from the middle of the grown ingot; (c) a projection reflection topograph of the wafer area marked by the rectangle in (b), 000ℓ reflection, $2\theta \sim 150°$.

The seed used for this growth includes some crystallites and cracks at its periphery. During the growth, these defects partially disappear in the first millimetres of growth. But some other large cracks occur in the upper part of the ingot. Most of these cracks, indicated on figure 6, are located in the zone opposite to the facet which is perpendicular to the inclined *c*-axis, showing the asymmetry of the growth.

Defect propagation. Figures 7(a) and (b) show optical transmission micrographs recorded using the polarizing microscope with a crossed analyser of a 8° off-axis seed wafer and of a wafer cut from the middle of a 4H-SiC ingot grown from this seed, respectively. The good-quality seed wafer includes a few micropipes and cracks mainly located towards its right-hand side; see figure 7(a). The wafer cut from the middle of the new grown crystal indicates clearly the enlargement of the ingot lateral size with respect to that of the seed. The enlargement is mainly produced by the reorientation of crystallites of the polycrystals growing around the main crystal and their incorporation into it. The quality of this new enlarged crystal is not very good; many micropipes and cracks can be observed at the wafer periphery, while its central part is nearly defect free. The small black spots present on the micrographs correspond to the carbon particles deposited during the growth. The inclusion of another polytype formed during the crystal growth is located at the lower right corner of figure 7(b). Figure 7(c) is the projection reflection topograph of the wafer area marked in figure 7(b) by the rectangle. Various defects can be detected, such as micropipes (white spots) Krishna *et al* (1985), Huang *et al* (1999), Dudley and Huang (2000), diagonal cracks on the left and distortions associated with the inclusion on the right-hand side of the image. These investigations, using both optical transmission microscopy and projection topography techniques, are possible only after ingot slicing and subsequent polishing of wafer surfaces.

However, much useful information can be obtained without any preparation of as-grown ingots using the section topography technique. Figure 8 presents a set of the section topographs of the ingot grown from the seed shown in figure 7(a), recorded using four different geometries shown in figure 2. The horizontal and vertical sections, figures 8(a), (b) and (c), (d), respectively, correspond approximately to the central part of the ingot. For the sake of simplicity, the sections recorded at various heights of the incident beam on the ingot are

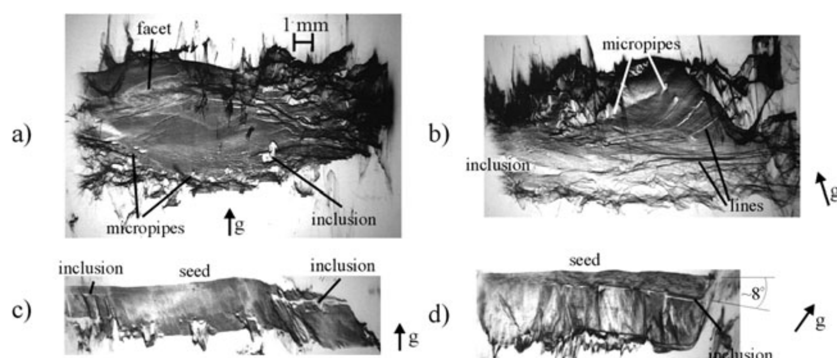

Figure 8. Section topographs (a)–(d) of the ingot grown from the seed wafer of figure 7(a) recorded for four different experimental geometries represented in figures 2(a)–(d), respectively. The inclusion marked in the optical micrograph of figure 7(b) is indicated also in figure 8(a). The vector $\boldsymbol{g}$ is the projection of the diffraction vector on the film.

not presented. Due to the geometrical projection onto the film, the horizontal sections have an elliptical shape, while the cross-section where the incident beam meets the sample is circular. The presence of the polycrystal surrounding the main crystal leads to deformation of the ellipse and produces additional contrast at the periphery of the ingot.

The sample volume diffracting to create the image of figure 8(a) corresponds roughly to the wafer shown in figure 7(b). There is an inclusion in the lower right part of the topograph, apparently the same one as in figure 8(b). Many micropipes appear, mainly in the lower left part of the image; however, the central part of the ingot remains nearly defect free. The facet, i.e. the natural surface perpendicular to the c-axis, observed as a light elliptical feature in the upper left region of the section, corresponds to a part of crystal with elevated crystalline quality. Defects similar to the inclusions or micropipes are revealed in figure 8(b), which is the horizontal section topograph recorded with the ingot turned by 90° around its vertical axis with respect to the position of the crystal in figure 8(a). The sections of figures 8(a), (b) both correspond to the 000ℓ reflections. However, an additional feature is observed on figure 8(b): the lines nearly perpendicular to the diffraction vector projection $\boldsymbol{g}$. The lines are curved if the crystal matrix is deformed, they can show either white or black contrast and their density is higher when closer to the seed. The corresponding distortion of 000ℓ reflecting planes is shown schematically in figure 9 for the four geometries used. The lines can be observed only if the projection of the c-axis and the diffraction vector on the film are approximately perpendicular; see figures 8(b) and 9(b).

The vertical section topographs recorded with the incident beam parallel to the main vertical axis of the cylindrical ingot allow one to follow the crystal growth from the seed to its natural top surface. In both vertical sections, figures 8(c), (d), the seed–crystal interface is hardly visible, indicating a smooth start to the crystal growth. The vertical sections recorded with the projection on the film along the c-axis and the projection of the diffraction vector nearly parallel (perpendicular)—see figure 8(c), (figure 8(d))—show the crystal with good (poor) crystalline quality, at least at its central part. Two inclusions of other polytypes, 6H-SiC or 15R-SiC, near to the seed can be observed in figure 8(c), the one on the right of the image corresponding to the periphery of the ingot, while the second one, towards the left of the image, is located closer to the central part of the crystal. The section in figure 8(d) was recorded approximately at the level of the SiC inclusion on the left of figure 8(c). Figure 8(d) indicates that this inclusion starts to grow from one side of the ingot and propagates at the

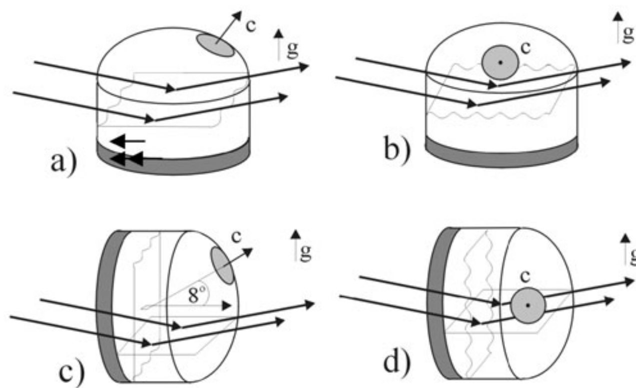

Figure 9. Schematic drawings of the observed distortion of the reflecting planes with respect to the *c*-axis direction for the four geometrical set-ups used, in the geometries of figures 2(a), (b), (c) and (d), respectively.

angle of 8° with respect to the horizontal ingot axis until it reaches the other side of the ingot. The inclusion leads to many planar defects growing parallel to the vertical ingot axis up to the natural crystal surface. These planar defects are what leads to the observation of the lines in figure 8(b). The systematic investigation of several 4H-SiC ingots indicates that these 6H inclusions at 8° occasionally appear and are generally reversible. The defects generated are often only in part of the crystal; however, they considerably degrade its crystalline quality. This polytype switching originates from the 8° off-axis orientation of the seed. If at the beginning of the growth process some instability appears, a 6H-SiC or 15R-SiC single-crystal grain can be created outside the seed. In the case where this grain is located at the right extremity of the seed and has the same orientation as the 4H main crystal, it starts to grow and progressively covers a part of the 4H crystal. If during the further crystal growth the process parameters such as pressure and temperature are favourable to the growth of the 4H polytype, the conversion back to 4H-SiC appears. However, this re-conversion leads to the appearance of distortions in the new grown crystal, such as grain boundaries.

4. Summary and conclusions

The occurrence and propagation of the defects occurring during the growth of 4H-SiC crystals was investigated using mainly optical microscopy and x-ray section topography techniques in transmission mode. Thanks to the high flux and high energy of the x-ray beams available at the ESRF, together with the large beam size, a very simple set-up could be used to study the whole volume of the ingots with a diameter up to 50 mm.

By combining x-ray topography and optical microscopy, we have shown that the quality of the SiC ingots grown by the modified Lely method depend considerably of the quality and the polarity of the seed. The enlargement of the ingots is due to the alignment of the polycrystal during the growth. Finally, some systematic analysis of the ingots and the slices has shown the occurrence of some inclusions of another polytype which degrade the crystalline quality and lead to some distortion such as grain boundaries.

References

Anikin M and Madar R 1997 *Mater. Sci. Eng.* B **46** 278

Authier A, Lagomarsino S and Tanner B K 1996 *X-ray and Neutron Dynamical Diffraction: Theory and Applications (NATO ASI Series)* (Berlin: Springer) pp 89–99

Baruchel J, Epelboin Y, Gastaldi J, Hartwig J, Kulda J, Rejmankova P, Schlenker M and Zontone F 1994 *Phys. Status Solidi* a **141** 59–69

Chourou K, Anikin M, Bluet J M, Lauer V, Guillot G, Camassel J, Juillaguet S, Chaix O, Pons M and Madar R 1998 *Mater. Sci. Forum* **264–268** 17–20

Dudley M and Huang X 2000 *Mater. Sci. Forum* **338–342** 431–6

Frank F C 1951 *Acta Crystallogr.* **4** 497–501

Heindl J, Strunk H P, Heydemann V D and Pensl G 1997 *Phys. Status Solidi* a **162** 251–62

Huang X R, Dudley M, Vetter W M, Huang W, Wang S and Carter C H 1999 *Appl. Phys. Lett.* **74** 353–5

Krishna P, Jiang S S and Lang A R 1985 *J. Cryst. Growth* **71** 41–56

Madar R, Anikin M, Chourou K, Labeau M, Pons M, Blanquet E, Dedulle J M, Bernard C, Milita S and Baruchel J 1997 *Diamond Relat. Mater.* **6** 1249–61

Milita S, Madar R, Baruchel J and Mazuelas A 1998 *Mater. Sci. Forum* **264–268** 29–32

Moulin C, Pons M, Pisch A, Grosse P, Faure C, Basset G, Passero A, Billon T, Pelissier B, Anikin M, Pernot P and Madar R 2001 *Mater. Sci. Forum* **353–356** 7–10

Müller St G, Glass R C, Hobgood H M, Tsvetkov V F, Brady M, Henshall D, Jenny J R, Malta D and Carter C H Jr 2000 *J. Cryst. Growth* **211** 325–32

Schulze N, Barrett D L, Pensl G, Rohmfeld S and Hundhausen M 1999 *Mater. Sci. Eng.* B **61–62** 44–7

Tairov Yu M and Tsvetkov V F 1978 *J. Cryst. Growth* **43** 208

Tsvetkov V F *et al* 1998 *Mater. Res. Soc. Symp. Proc.* **512**